Analyst

Accepted Manuscript

This article can be cited before page numbers have been issued, to do this please use: R. Guo, S. Hu and Z. Wang, *Analyst*, 2020, DOI: 10.1039/D0AN00678E.

ROYAL SOCIETY OF CHEMISTRY

rsc.li/analyst

View Article Online
DOI: 10.1039/D0AN00678E

ARTICLE

A portable electrochemiluminescence bipolar electrode array for the visualized sensing of Cas9 activity

Received 00th January 20xx,
Accepted 00th January 20xx

DOI: 10.1039/x0xx00000x

Rui Guo, [a] Shanwen Hu*[b], Zonghua Wang*[a]

CRISPR/Cas9 has already become a powerful tool for genomic manipulation, and the evaluation of Cas9 activity is essential for the precise control of the CRISPR system. Herein we develop a point-of-care platform for rapid and visible determination of Cas9 activity. A bipolar electrochemiluminescence (ECL) biosensor platform consists of an Au electric circuit fabricated on a glass substrate and a PDMS layer act as reservoirs. DNA probes are modified on electrode and hybridization chain reaction (HCR) is applied to introduce ferrocene labeled DNA. The CRISPR/Cas9 system can recognize the immobilized DNA probes and cleave them from the electrode surface, as well as the labeled H1 and H2, so the cleavage activity is closely related to the labeled ferrocene. The modified electrode is embodied in a closed bipolar system, so that the oxidation reaction on sensing poles could be detected by the anodic ECL reactions on isolated luminescent poles due to charge balance, leading to the changes of ECL signals. This portable, integrated and convenient platform turns Cas9 activity into visible color changes, which is meaningful for the discovery of a new CRISPR/Cas9 system or additional Cas9 inhibitors.

Introduction

Clustered Regularly Interspaced Palindromic Repeats (CRISPR) with CRISPR-associated (Cas) proteins are extensively used worldwide for its ability of gene editing and manipulation. [1] Among them, the associated proteins 9 (Cas9) mediated system is mostly used for the capability of targeting specific DNA sequence and induce site-specific break. which is closely related with Cas9 activity.[2] The success of gene editing relies on precise control of the manipulation process. In Cas9 based genome-editing assay, Cas9 can specifically bond with target DNA at designed location in guidance of sgRNA, and break the double strands. However, it is laborious and time-consuming to evaluate the Cas9 activity, as well as the cleavage working efficiency. Typically, researchers addressed this problem by using PCR assays after the target cell transfections and cultures. This process will take 8−14 days, and will be complicated by the laborious procedures. Radioisotope-labeled gel electrophoreses have become a standard prior method for analyzing off-target effects. Though numerous efforts been devoted to this issue, [3] the reported methods are still far from ideal, which limits the exploration of new CRISPR-Cas9 systems. Till now, the visualized sensing of Cas9 activity has not been realized yet, which is a momentous goal in CRISPR project, since it can give the intuitive reflection of the editing procedure directly through naked eyes.

Point-of-care testing (POCT) devices have experienced booming development over the past decade, offering advantages such as miniaturization, automation and on-site. They benefit public health worldwide especially in developing countries and show significant potential in clinical diagnosis and health evaluation.[4] The lack of sensitivity keeps POCT from quantitative detections. ECL has been widely used in biosensing for its overwhelming advantages, such as low background interference, simple operation process, high throughput, and visual imaging capability.[5, 6] The weak solubility of luminescent reagents in water and potential contaminations limit their biological applications. [7] Closed bipolar electrode (BPE) system with ECL as an analytical tool (BPE-ECL) is developed to solve this problem. [8] BPE is an electronic conductor in a solution when the power is supplied via driving sources without any electrical connection. The structure of BPE can be classified into open and closed while the function moles can be classified as the target at the same pole and target at the opposite pole with ECL reagents. The later one can divide the target with ECL reagents such as $Ru(bpy)_3^{2+}$ and luminol, avoiding the potential cross contaminations. ECL based BPE has been utilized for the determination of ATP[9], thrombin, biomarkers[10], drugs[11] and other biomolecules[12]. Xu's group developed a visual ECL ratiometry for the detection of prostate-specific antigen (PSA) on a closed BPE.[13] Zhang explained the mechanism of ECL in closed BPE and expand the scope of the detection target. [14, 15] Wang, etc. designed a useful nanoscale multi-channel bipolar electrochemistry platform for biosensing of CEA and AFP in serum. [16] Xing etc. designed an ECL based method for evaluating cleavage activity of the CRISPR/Cas9 system.[17] Liu etc. realized visual ECL sensing for cell surface glycoprotein by a BPE chip.[18] However, it is still challenging to detect Cas9 activity on ECL-BPE. The sensitivity is a limitation since concentrations of CRISPR reagents are low. Furthermore, Cas9 has no DNA recognition specificity without sgRNA, which means the whole CRISPR process should be executed on electrodes.

[a] College of Chemistry and Chemical Engineering, Shandong Sino-Japanese Center for Collaborative Research of Carbon Nanomaterials, Qingdao University, Qingdao, Shandong 266071, P. R. China
[b] Department of Health Inspection and Quarantine, School of Public Health, Fujian Medical University, Fuzhou, Fujian, 350122, P.R. China

View Article Online
DOI: 10.1039/D0AN00678E

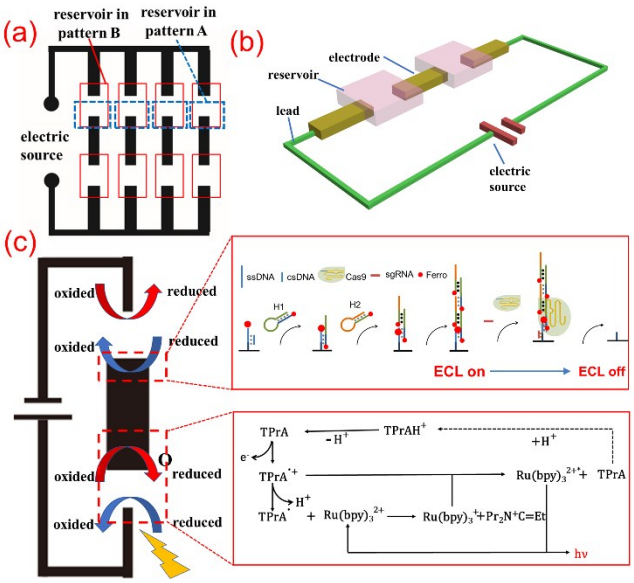

Scheme 1 illustration of the POCT platform and Mechanism of the visualized sensing of Cas9 Activity. (a) Diagram of the Closed BPE-ECL array. (b) Sketch for Au electric circuit and reservoirs. (c) General view of the CRISPR/Cas9 procedure and ECL signal generating mechanism.

Aiming at the visualized sensing of Cas9 activity, herein we proposed a new type of closed BPE-ECL system based on an Au electric circuit at a portable substrate as a POCT platform. A bipolar electrochemiluminescence (ECL) biosensor consists of an electrode array fabricated on a glass substrate and a PDMS layer act as a sample cell. DNA probes are modified on electrode and hybridization chain reaction (HCR) is applied to introduce ferrocene labeled DNA. The oxidation reaction on sensing poles could be detected by the anodic ECL reactions on isolated luminescent poles due to charge balance. The CRISPR/Cas9 system can recognize the probe DNA on the electrode and execute the cleavage process, which is closely related to the ECL signal, and induce visible color changes on the luminescent poles.

Experimental

2.1 Materials, equipment and apparatus

Polydimethylsiloxane (PDMS) materials including Sylgard 184 elastomer base and curing agent were gained from Dow Corning (Midland, MI). H_2SO_4, H_2O_2, KH_2PO_4, NaCl, KCl, ethylenediaminetetraacetic acid disodium salt (EDTA), ferrocene, dimethyl sulfoxide (DMSO), lead(Ⅱ) acetate trihydrate, were analytically pure grade from Sinopharm Chemical Reagent Co., Ltd (Shanghai, China) and used without any further purification. Tris(2,2'-bipyridine)dichlororuthenium(Ⅱ) hexahydrate, chloroplatinic acid and tripropylamine (TPrA) were purchased from Aladdin Biochemical Technology (Shanghai, China). Tris(2-carboxyethyl)phosphine hydrochloride (TCEP) was obtained from Sigma-Aldrich. Phosphate buffer saline (PBS) was obtained from Solarbio (Beijing, Chain). 1 M Tris-HCl and β-mercaptoethanol (MCH) were gained from Sangon Biotech. Co., Ltd. (Shanghai, China). ssDNA, csDNA, H1, H2, sgRNA, Cas9 nuclease, and Cas9 nuclease reaction buffer were obtained from Genscript (USA). Sequences of nucleic acid chains are listed as follows:

ssDNA: 5'-SH-TAA TGC GCC AGC CAA GCG CAC CTA ATT TTT GGT CGG CAC TTA ATA TAA CCT AGA AGA AGG TGT TTA AGT A -Ferrocene-3'

csDNA: 5'-GGT TAT ATT AAG TGC CGA CCA AAA ATT AGG TGC GCT TGG CTG GCG CAT TA-3'

sgRNA: 5'-GGU UAU AUU AAG UGC CGA CCA AAA AUU AGG UGC GCU UGG CUG GCG CAU UA-3'

H1: 5'-AGG GCG GGT GGG TGT TTA AGT TGG AGA ATT GTA CTT AAA CAC CTT CTT CTT GGGT-Ferrocene-3'

H2: 5'- Ferrocene- TGG GTC AAT TCT CCA ACT TAA ACT AGA AGA AGG TGT TTA AGT TGG GTA GGG CGG G-3'

2.2 Fabrication of POCT platform

This electric circuit is fabricated following a typical microlithography technique shown in Figure 1, Briefly, a designed electric circuit pattern was printed on film as a mask and pressed on the SG-2506 borosilicate glass. After being exposed to UV for 1min, the pattern on film was transferred to the photoresistor layer on the substrate. Then the substrate was subjected to 50 nm gold deposition by physical vapor deposition (PVD). Acetone was utilized to remove the remaining photoresistor as well as the Au layer on it, leaving a pattern of Au layer on Cr, followed by 1 min of soaking in chromium etchant to remove Cr without the protection of Au layer. A hollowed PDMS layer is covered on this electric circuit, the holes on PDMS layer act as reservoirs for reagent storage, and the Au layer exposed on the bottom of the reservoirs act as electrodes. PDMS layer with pattern A is covered on the substrate for the functionalization of electrodes and replaced by pattern B for ECL testing. In pattern B, the PDMS layer contains two holes for each BPE unit, one serves as a sensing pole and the other serves as the luminescent pole. This electric circuit with leads can be connected to an electrochemical workstation for CV and ECL spectra, and a battery for POCT detections.

2.3 Modification of sensing poles

The Au bipolar electrodes were washed with deionized water for 3 times and dried by flowing N_2. The following solutions were injected into the reservoirs. 10 μL 1 μM ssDNA in 1.0 M KH_2PO4 was incubated on the Au substrates for 2 h. Then the Au substrates were washed with deionized water for 3 times and dried by flowing N_2. 10 μL 1 mM β-mercaptoethanol (MCH), 10 μL 1 μM csDNA, 10 μL mixture of 1 μM H1 and H2 in TE-NaCl (10 mM Tris-HCl, 1 mM EDTA, 1 M NaCl), were sequentially injected to the reservoirs respectively. HCR process was executed for 1.5h at room temperature.

2.4 ECL testing

The anode solution contained 0.75 mM $[Ru(bpy)_3]^{2+}$, 25 mM TPrA, and 0.01 M PBS (pH=7.4). The cathode solution contained 1 M KCl, 0.1 M PBS and a little dimethyl sulfoxide (DMSO). The driving voltage range from 2 V-5 V, the scan rate was 100 mV/s while the voltage of PMT was 480 V.[19]

View Article Online
DOI: 10.1039/D0AN00678E

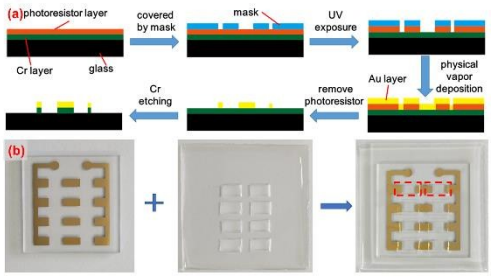

Figure. 1 (a) Schematic illustration of the Au electric circuit on a glass substrate. (b) Photograph of the Au electric and PDMS layer, the red square frames show the sample reservoirs.

2.5 Cleavage Assay triggered by CRISPR/Cas9 system

5 μL Cas9 Nuclease (1 μM final concentration) was first incubated with 5 μL 1 μM sgRNA (30 nM) in HEPES buffer (containing 20 mM HEPES, 100 mM NaCl, 5 mM $MgCl_2$, 0.1 mM EDTA, pH 6.5) and preincubated 10 min at 25 °C. Then the mixture was added to the electrodes and reacted for 1 h before the ECL signal was recorded.

Results and discussion

3.1 Mechanism of the Closed BPE-ECL POCT platform

As illustrated in Scheme.1, this POCT platform consists of an Au electric circuit on a glass substrate, and a hollowed PDMS layer covers on it. Au electric circuit is stable enough for further analysis since the Au atoms deposited by PVD is solid on Cr. The PDMS chip can fit with the Au layer to prevent fluid leaking, to make two physically separated electrochemical cells, one serves as a sensing pole and the other serves as the luminescent pole, with BPE as the only current path between the cells. In this electric circuit, since only electronic current can travel through two poles of the closed BPE, the charge balance follows not only in the two BPE poles, but also exists in the whole closed-loop circuit theoretically, which means the oxidation reaction on sensing poles could be detected by the anodic ECL reactions on isolated luminescent poles. [14] This gives us opportunities to isolate the ECL reagents with the biosensing system to avoid potential contaminations. As reported by Zhang's work, under a certain condition, the voltammetric response of the bipolar electrode system has a similar sigmoidal shape as a conventional two- or three-electrode system.

The ECL signal is generated on electrooxidation of $[Ru(bpy)_3]^{2+}$, a typical phosphorescent material as an ECL label, and TPrA as a co-reactant. The detailed ECL mechanism in a traditional three-electrode system was proposed by Bard's group. [20] On this POCT platform, closed BPE-ECL sensing units are integrated. Each unit contains a luminescent pole using $Ru(bpy)_3^{2+}$ and TprA as ECL reagents, as well as an isolated sensing pole with modified electrode and high ionic strength electrolyte. Figure 2 is the corresponding ECL signal and CV curve when the anodic ECL reagents ($Ru(bpy)_3^{2+}$ /TprA, 5 mM/25 mM) were filled in the luminescent pole. A typical ECL signal was generated on this closed BPE-ECL sensing unit.

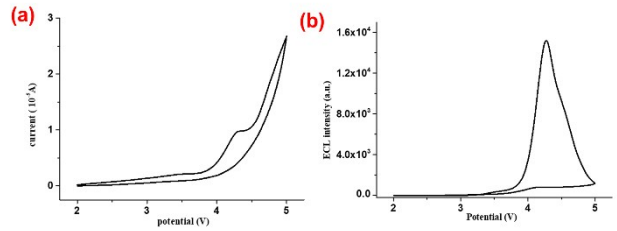

Figure. 2. (a) CV spectrum on the ECL-BPE. (b) The ECL-potential curve of the ECL-BPE. ECL detection buffer: 0.01M PBS (pH=7.4) contained 0.75 mM $[Ru(bpy)_3]^{2+}$ and 25 mM TPrA.

As shown in Scheme.1c, the ECL intensity in the luminescent pole is closely related to the oxidization reactions on the decorated electrode, showing the possibility to monitor the immobilized Ferro by ECL signals. Four pairs of closed-BPE are integrated as a model of array detection on chip.

The CRISPR/Cas9 system is designed according to reported works. [17] The sgRNA can help to recognize the target sequences and bond to the dsDNA as a complex with Cas9. As long as the cleavage happens, the ferrocene on the electrode will change and affect the electric signal, which eventually affects the ECL signal. By this means, we developed a connection between ECL signal and Cas9 activities.

3.2 Optimization of the ECL testing on chip

To gain the best ECL performance as initial signal, we firstly optimized the ECL detecting conditions. Results show the ECL signal can be influenced by concentrations of reagents. An optimized condition of $Ru(bpy)_3^{2+}$/TprA = 5 mM/25 mM is utilized for further detecting. The electric conditions on the sensing port can also affect the initial signal. The ssDNA on the electrode is a key factor to be optimized. The signal increased and reached a peak of 1.0 μM. The pH in luminescent poles will also influence the ECL performance, signals in the neutral buffer are stronger than others, so pH=7.4 is chosen as an optimized condition.

3.3 The HCR process for signal enhancement

Nucleic Acid Amplification Strategies can be integrated with ECL biosensors to get enhanced signals.[21-23] Since the electrochemistry reactions on sensing poles reflect ECL reactions, the amount of ferrocene on electrodes is essential for the ECL signal. In order to improve the modification amount of ferrocene, a hybridization chain reaction (HCR) is designed on the electrode.

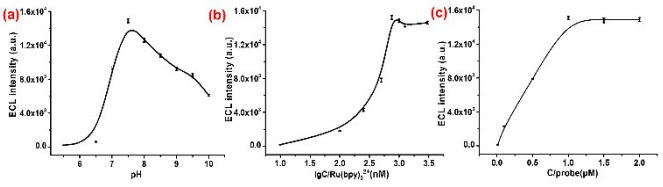

Figure. 3 Optimization of the ECL testing on chip. (a) ECL signals change with pH in the luminescent pole; (b) ECL signals change with concentrations of $[Ru(bpy)_3]^{2+}$ in the luminescent pole; (c) ECL signals change with concentrations of ssDNA during decoration.

View Article Online
DOI: 10.1039/D0AN00678E

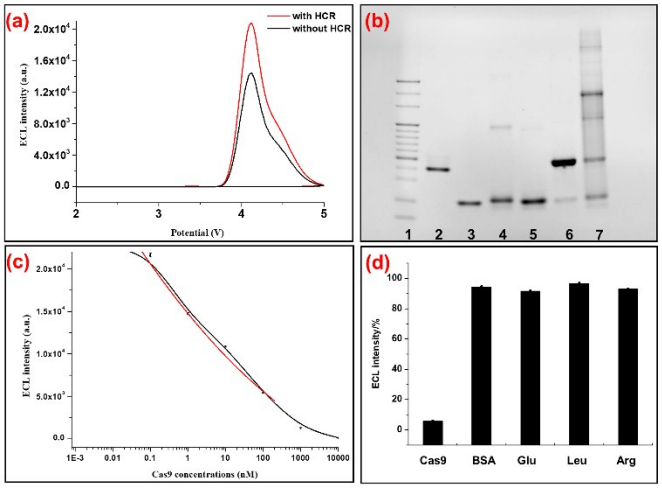

Figure. 4 (a) ECL curves with or without the HCR process. (b) Characterization of HCR product using native PAGE: lane 1, 20 bp makers; lane 2, 1.0 μM ssDNA; lane 3, 1.0 μM csDNA; lane 4, 1.0 μM H1; lane 5, 1.0 μM H2; lane 6, 1.0 μM ssDNA+csDNA; lane 7, 1.0 μM ssDNA+csDNA+H1+H2; (c) The linear fitting curve of ECL signals changing with concentrations of Cas9. (d) ECL signals after 1 μM samples added to the sensing poles.

The immobilized ssDNA serves as the initiator and triggered cascade reactions of HCR. As shown in Scheme 1, the opened ssDNA exposes another toehold which could bind the overhang of hairpin 1 (H1). Then hairpin 2 (H2) hybridizes with the exposed toehold of H1 followed by a disassembly step in which the initiator is displaced from the H1-H2 complex. The reactions of HCR were validated separately via native polyacrylamide gel electrophoresis (PAGE). Lane 1 represents the ladder. Clear bands were observed for ssDNA, csDNA, H1, and H2, respectively (lane 2, 3, 4 and 5). In lane 6, ssDNA is incubated with csDNA, and a new band appeared, indicating the formation of dual strands complex. In lane 7, after H1 and H2 were mixed with ssDNA and csDNA, hybridization products appeared, resulted in new bands with longer sequences. Typical trailing bands of HCR products were witnessed. It should be noted that the band represents dual strands complex of ssDNA and csDNA was much weaker than in lane 6 since it participates in the HCR reactions.[24]

More and more H1 and H2 participates the HCR reactions and were immobilized on electrodes during the HCR process, meanwhile, the amount of labelled ferrocene immobilized on electrodes was also improved. After the HCR process, the electrodes show an outstanding ECL property. As shown in Figure 4a. the ECL signals were remarkably improved, resulting in an enhanced initial signal, which will be beneficial for the following off-based biosensing.

3.4 Biosensing of Cas9 Activity on chip

The CRISPR/Cas9 reactions can be detected on this chip since the cleavage process will affect the amount of immobilized ferrocene. As a model assay, the cleavage efficiency here is changed via the concentration of Cas9. As shown in Figure 4c, the introduction of

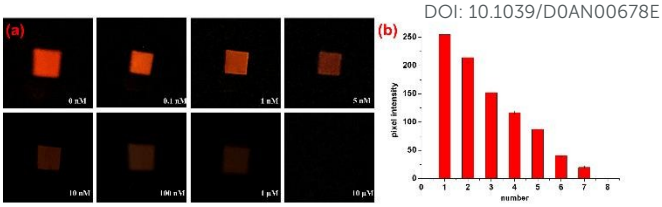

Figure. 5 (a) ECL images on luminescent poles with increased concentrations of Cas9. (b) pixel intensity of red color in each image.

Cas9-sgRNA in sensing poles can significantly reduce the ECL signal in luminescent poles. Furthermore, the reduction of ECL signal increases with Cas9 concentrations arise. A linear response can be found at a range of 0.1 nM-100 nM, while the limit of detection was 0.01nM. To evaluate the selectivity of this biosensing platform, different biomolecules including BSA, glutathione, leucine, and arginine at the same concentration of 1 μM are added to the sensing pole. Negligible signal loss is witnessed while Cas9 at the same concentration can efficiently decrease the ECL signal, showing the signal can be selectively related to Cas9 activities.

3.5 Visualized sensing of Cas9 Activity on POCT

A portable ECL-BPE makes an ideal POCT platform possessing features such as high sensitivity, user-friendly and cheap.[25, 26] Battery-triggered chip allows the platform to work away from power sources while the visual detection avoids the need of signal readers.[27, 28] Herein, we were amazed to find the change of ECL signal is strong enough to be witnessed by naked eyes. Inspired by this phenomenon, we drive this chip by battery to make a portable device as a POCT model. As shown in Figure 5, triggered by a 4V battery, the chip shows visible color changes while the Cas9 concentration is 0 nM, 0.1 nM, 1 nM, 5nM, 10 nM, 100 nM, 1 μM, and 10 μM. The color changes of images are characterized by the solution visualization analysis.[29] Pixel intensity of red color in each image is captured by Image-Pro Plus (IPP) program, a clear gradient can be witnessed in Figure 5b, corresponding to the ECL curves. These results demonstrate this chip to be a feasible and promising platform for visualized sensing of Cas9 activity.

Conclusions

In summary, a closed BPE-ECL based POCT platform containing two isolated poles is proposed to determine Cas9 activity in the CRISPR project. In the luminescent pole, the ECL signal was generated with $[Ru(bpy)_3]^{2+}$ and TPrA, while in the sensing pole, the CRISPR/Cas9 reactions took place. The oxidation reaction on sensing poles could be detected by the anodic ECL reactions, and the signal is improved by HCR. POCT model was successfully carried out with visible results. Considering the importance of Cas9 activities in CRISPR projects, this convenient, portable and visualized platform may introduce a great improvement in work efficiency.

Conflicts of interest

There are no conflicts to declare.

Acknowledgments

We gratefully acknowledge the National Natural Science Foundation (Grants 21804064) of China. This work was also supported by A Project of Shandong Province Higher Educational Science and Technology Program (J18KA083), Natural Science Foundation of Shandong Province (2018GGX102030) and Taishan Scholar Program of Shandong Province (ts201511027).

Notes and references

1 M.R. O'Connell, B.L. Oakes, S.H. Sternberg, A. East-Seletsky, M. Kaplan, J.A. Doudna, *Nature*, 2014, **516**, 263-266.
2 H.X. Wang, M. Li, C.M. Lee, S. Chakraborty, H.W. Kim, G. Bao, *Chem. Rev.*, 2017, **117**, 9874-9906.
3 K.J. Seamon, Y.K. Light, E.A. Saada, J.S. Schoeniger, B. Harmon, *Anal. Chem.*, 2018, **90**, 6913-6921.
4 H. Motaghi, S. Ziyaee, M.A. Mehrgardi, A.A. Kajani, A.K. Bordbar, *Biosens. Bioelectron.*, 2018, **118**, 217-223.
5 Zou, Z. Wang, H. Zhang and Y. Liu, *Biosens. Bioelectron.*, 2018, **122**, 205-210.
6 H. Zhang, Z. Wang, Q. Zhang, F. Wang and Y. Liu, *Biosens. Bioelectron.*, 2019, **124-125**, 184-190.
7 M.R. Moghaddam, S. Carrara, C.F. Hogan, *Chem. Commun.*, 2019, **55**, 1024-1027.
8 Y.Z. Wang, C.H. Xu, W. Zhao, Q.Y. Guan, H.Y. Chen, J.J. Xu, *Anal. Chem.*, 2017, **89**, 8050-8056.
9 X.W. Zhang, R.A. Lazenby, Y. Wu, R.J. White, *Anal. Chem.*, 2019, **91**, 11467-11473.
10 Q. F. Zhai, X. W. Zhang, Y. Xia, J. Li and E. K. Wang, *Analyst*, 2016, **141**, 3985-3988.
11 L.S. Jin, J.T. Qiao, J.H. Chen, N. Xu, M.S. Wu, *Talanta*, 2020, **208**, 8.
12 W. Xu, K. Y. Fu, C. X. Ma and P. W. Bohn, *Analyst*, 2016, **141**, 6018-6024.
13 H.J. Lu, W. Zhao, J.J. Xu, H.Y. Chen, *Biosens. Bioelectron.*, 2018, **102**, 624-630.
14 J.D. Zhang, L. Lu, X.F. Zhu, L.J. Zhang, S. Yun, C.S. Duanmu, *ACS Sens.*, 2018, **3**, 2351-2358.
15 J.D. Zhang, N. Hao, L. Lu, S. Yun, X.F. Zhu, K. Hong, *J. Electroanal. Chem.*, 2019, **832**, 1-6.
16 Q.F. Zhai, X.W. Zhang, Y.C. Han, J.F. Zhai, J. Li, E.K. Wang, *Anal. Chem.*, 2016, **88**, 945-951.
17 W. Liu, H. Yu, X. Zhou, D. Xing, *Anal. Chem.*, 2016, **88**, 8369-8374.
18 Z. Tian, L. Mi, Y. Wu, F. Shao, M. Zou, Z. Zhou and S. Liu, *Anal. Chem.*, 2019, **91**, 7902-7910.
19 H. Zhang, Z. Wang, F. Wang, Y. Zhang, H. Wang and Y. Liu, *Anal. Chem.*, 2020, **92**, 5546-5553.
20 W. Miao, J.P. Choi, A.J. Bard, *J. Am. Chem. Soc.*, 2002, **124**, 14478-14485.
21 X.Y. Ma, H.R. Xu, K. Qian, M. Kandawa-Schulz, W.M. Miao, Y.H. Wang, *Talanta*, 2020, **208**, 120441.
22 G.T. Jie, Q. Zhou, G.F. Jie, *Talanta*, 2019, 194, 658-663.
23 M. S. Wu, N. Xu, J. T. Qiao, J. H. Chen and L. S. Jin, *Analyst*, 2019, **144**, 4633-4638.
24 Y. Gu, J. Song, M. X. Li, T. T. Zhang, W. Zhao, J. J. Xu, M. Liu and H. Y. Chen, *Anal. Chem.*, 2017, **89**, 10585-10591.
25 R. Liu, C.S. Zhang, M. Liu, *Sens. Actuators B: Chem.*, 2015, **216**, 255-262.
26 L. Chen, C.S. Zhang, D. Xing, *Sens. Actuators B: Chem.*, 2016, **237**, 308-317.
27 M. Liu, D. Wang, C.L. Liu, R. Liu, H.J. Li, C.S. Zhang, *Sens. Actuators B: Chem.*, 2017, **246**, 327-335.
28 C.L. Liu, D. Wang, C.S. Zhang, *Sens. Actuators B: Chem.*, 2018, **270**, 341-352.
29 S.W. Hu, B.Y. Xu, W.K. Ye, X.H. Xia, H.Y. Chen, J.J. Xu, *ACS Appl. Mater. Interfaces*, 2015, **7**, 935-940.

View Article Online
DOI: 10.1039/D0AN00678E

Graphical Abstract

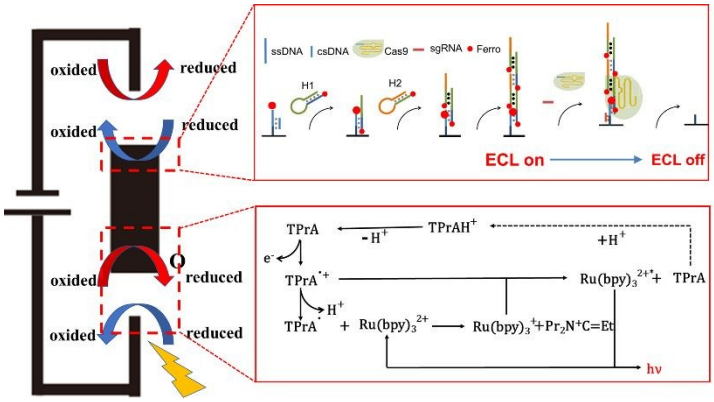

A new type of closed BPE-ECL system based on an Au electric circuit at a portable substrate is designed for the visualized sensing of Cas9 Activity in CRISPR/Cas9 system.